Supporting Information

Photoactivated Transition Metal Dichalcogenides to Boost Electron Extraction for All-Inorganic Tri-Brominated Planar Perovskite Solar Cells

Qingwei Zhou,[a] Jian Du,[a] Jialong Duan,[a] Yudi Wang,[a] Xiya Yang[a] Yanyan Duan[b] and Qunwei Tang*[a,c]*

[a] Institute of New Energy Technology, College of Information Science and Technology, Jinan University, Guangzhou 510632, PR China;
[b] State Centre for International Cooperation on Designer Low-Carbon and Environmental Material (SCICDLCEM), School of Materials Science and Engineering, Zhengzhou University, Zhengzhou 450001, PR China;
[c] Joint Laboratory for Deep Blue Fishery Engineering, Qingdao National Laboratory for Marine Science and Technology, Qingdao 266237, PR China.

E-mail: duanjialong@jnu.edu.cn; tangqunwei@jnu.edu.cn

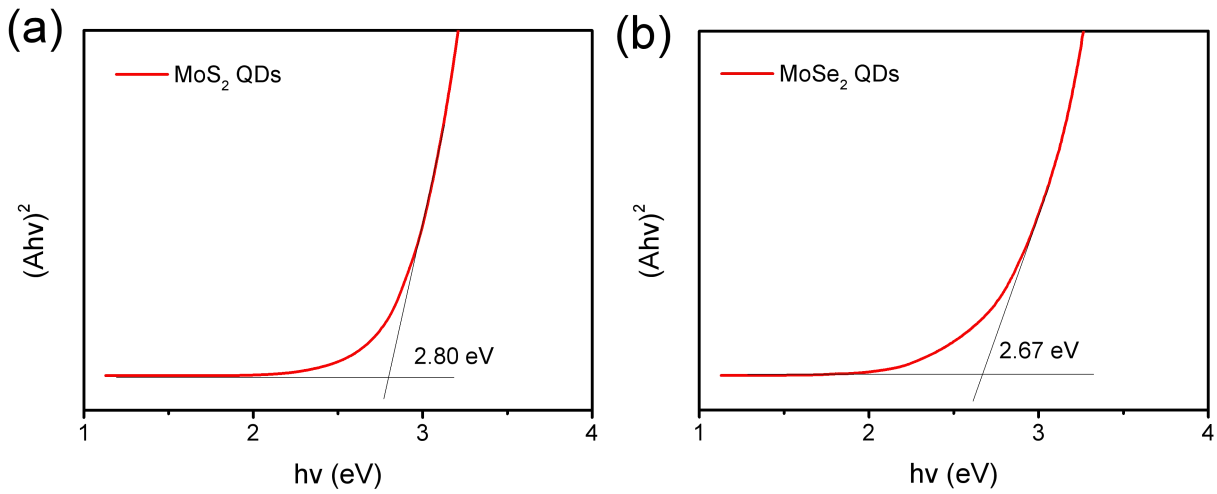

Fig. S1 UV-vis spectra of (a) MoS_2 QDs and (b) $MoSe_2$ QDs.

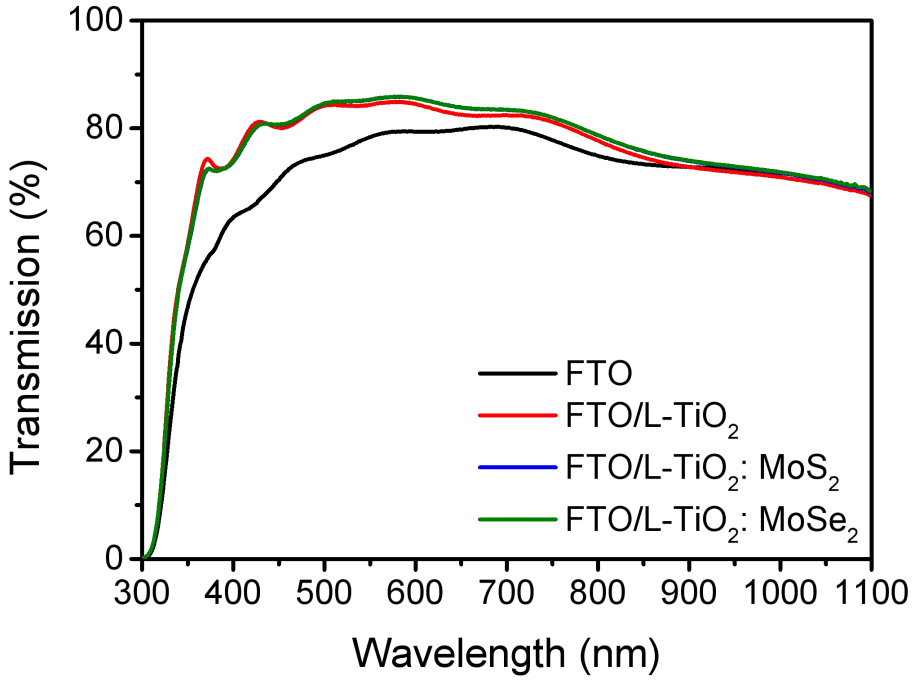

Fig. S2 Transmission spectra of FTO, FTO/L-TiO_2, FTO/L-TiO_2:MoS_2 and FTO/L-TiO_2:$MoSe_2$.

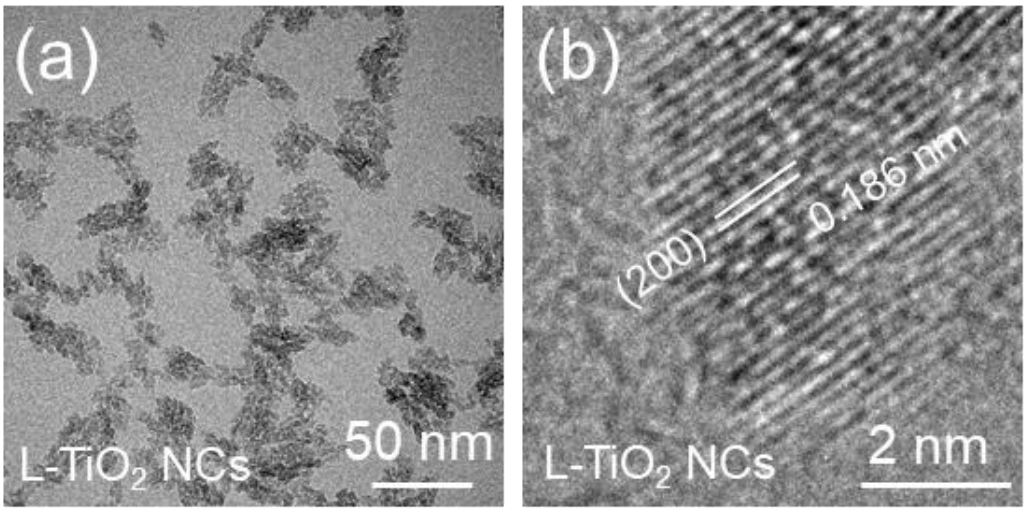

Fig. S3 (a) TEM and (b) HRTEM images of L-TiO_2 nanocrystals.

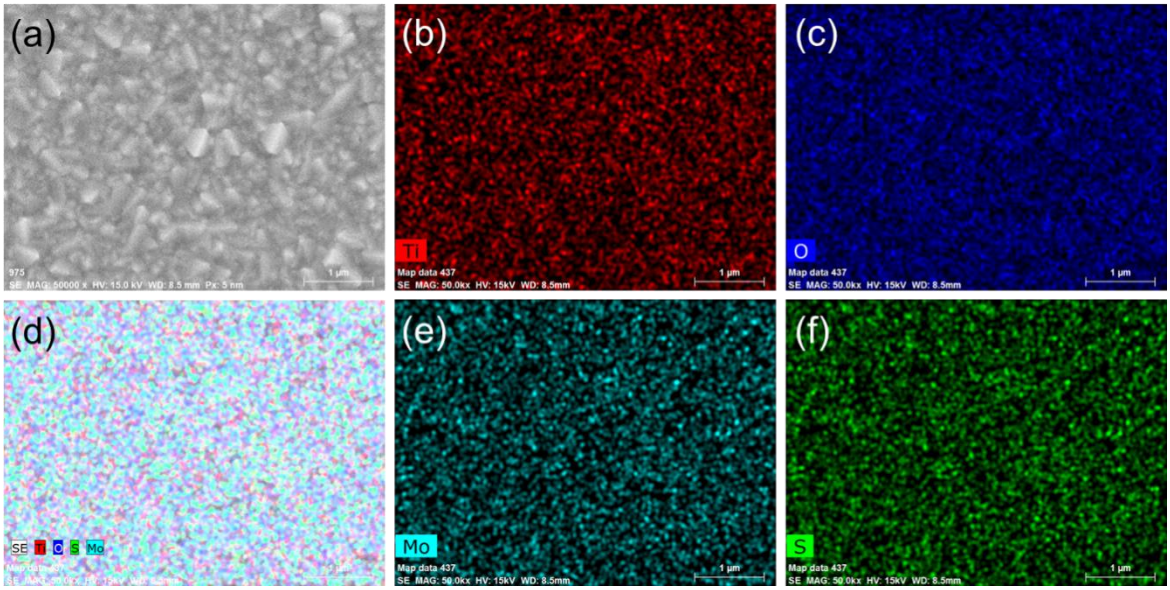

Fig. S4 EDS mapping images for L-TiO_2:MoS_2 film.

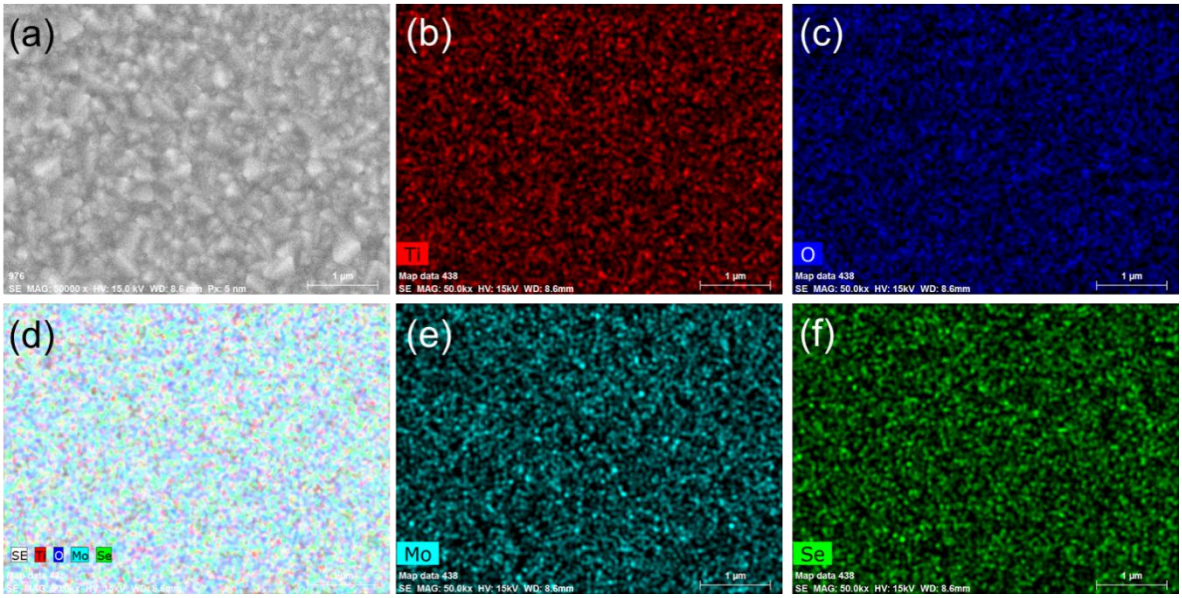

Fig. S5 EDS mapping images for L-TiO_2:$MoSe_2$ film.

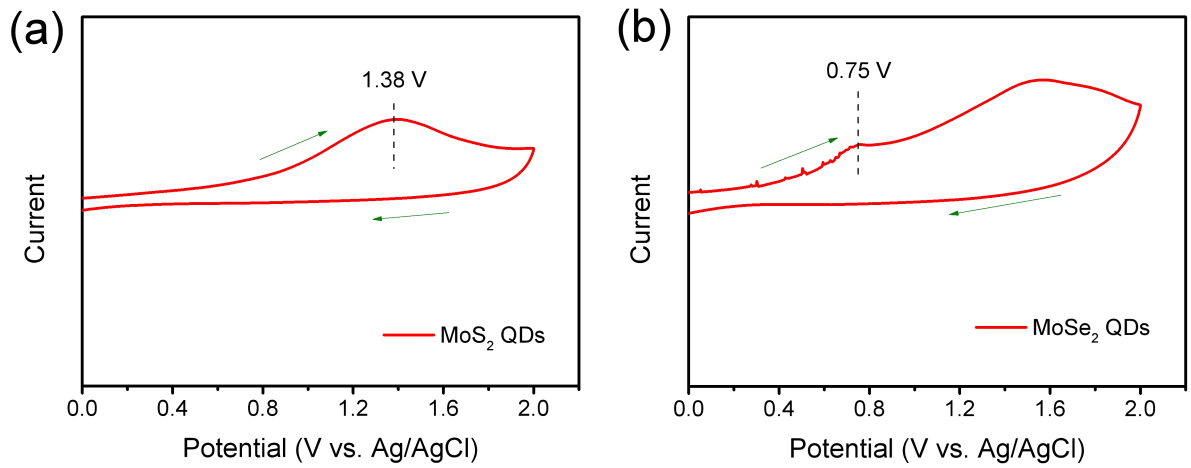

Fig. S6 CV curves of (a) MoS_2 QDs and (b) $MoSe_2$ QDs.

According to E_{VB} = -(4.4 + $E_{ox,onset}$) eV, where $E_{ox,onset}$ represents the oxidation potential, the VB are determined to be -5.78 and -5.15 eV for MoS_2 and $MoSe_2$ QDs, respectively. According to their optic band gap (Fig. S1), The CB of MoS_2 and $MoSe_2$ QDs are determined to be -2.98 and -2.48 eV, respectively, which is higher than that of TiO_2 (~ -4.0 eV).

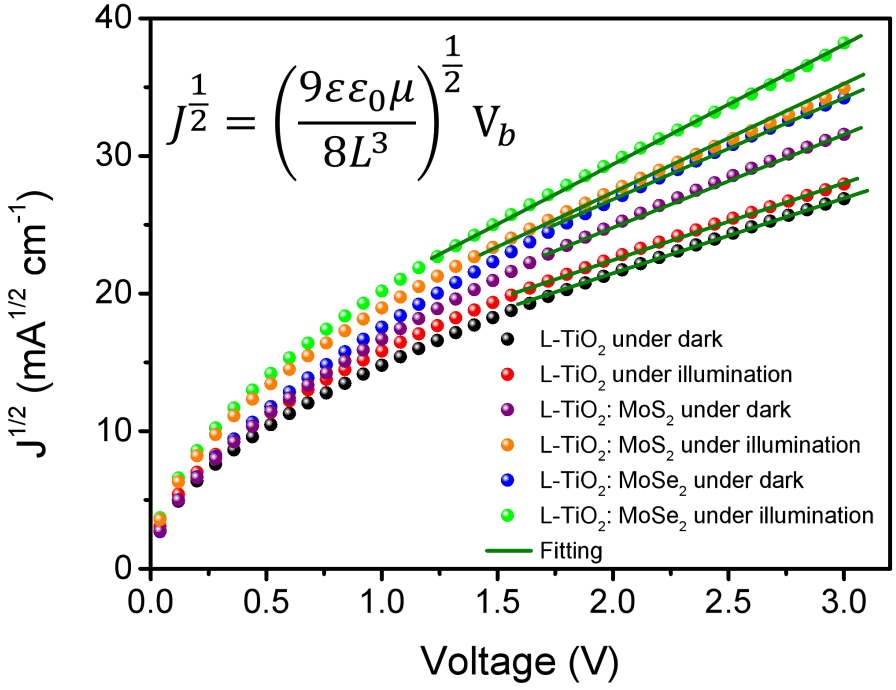

Fig. S7 Electron mobility for L-TiO_2, L-TiO_2:MoS_2 and L-TiO_2:$MoSe_2$ ETLs under different conditions using the SCLC model.

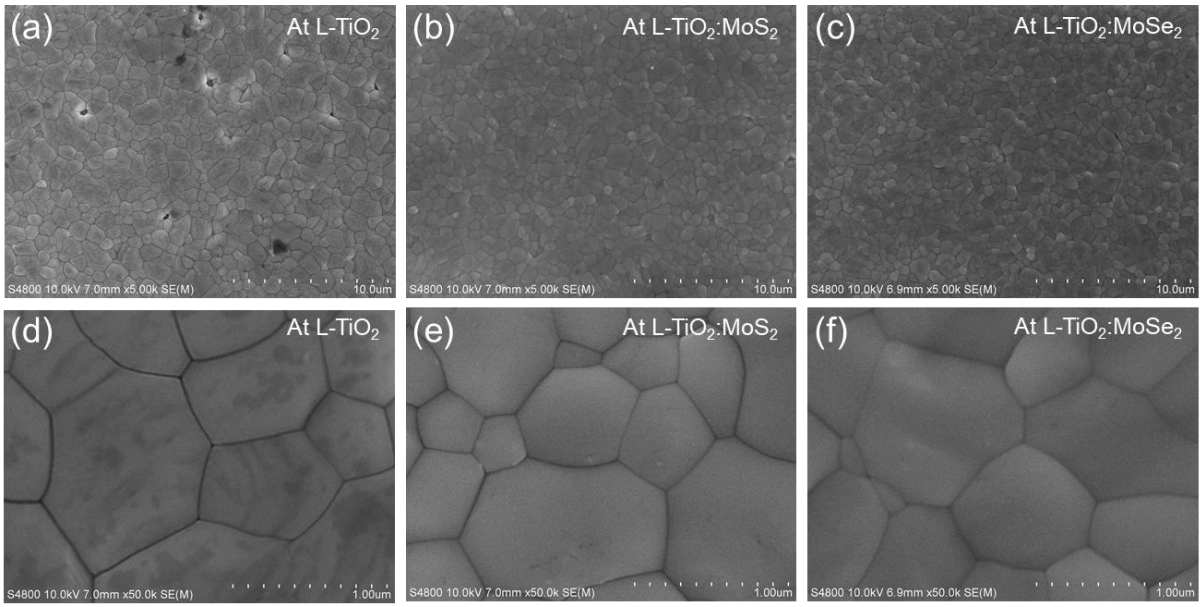

Fig. S8 SEM images of the $CsPbBr_3$ films fabricated on the surface of (a, d) L-TiO_2, (b, e) L-TiO_2:MoS_2 and (c, f) L-TiO_2:$MoSe_2$ ETLs.

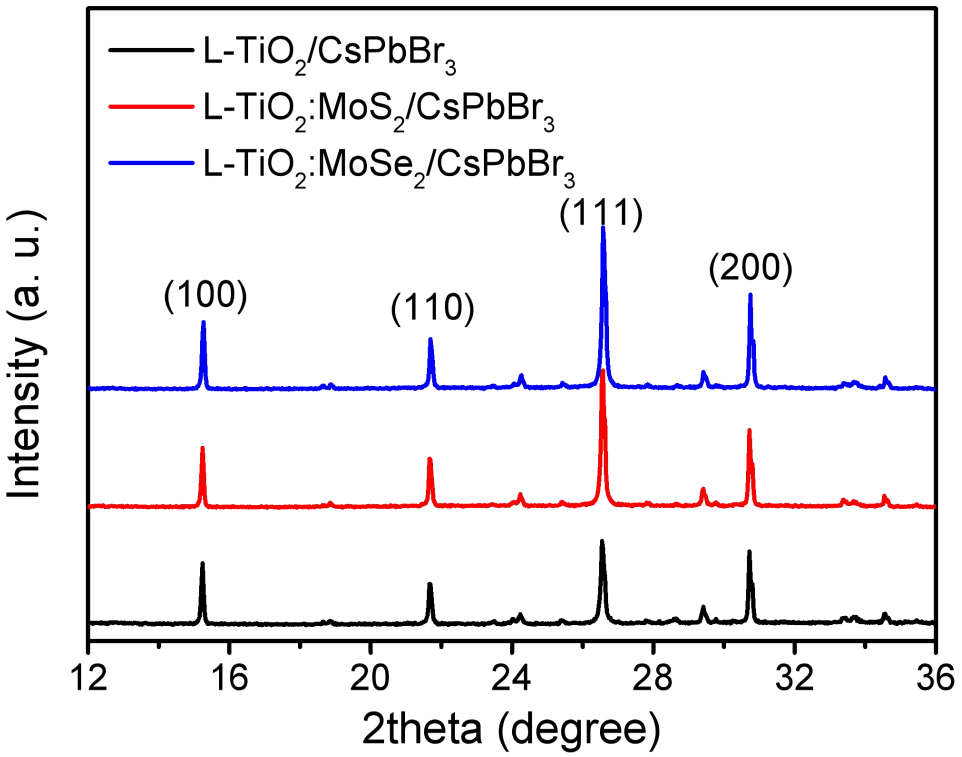

Fig. S9 XRD patterns of $CsPbBr_3$ films fabricated on the surface of L-TiO_2, L-TiO_2:MoS_2 and L-TiO_2:$MoSe_2$ ETLs.

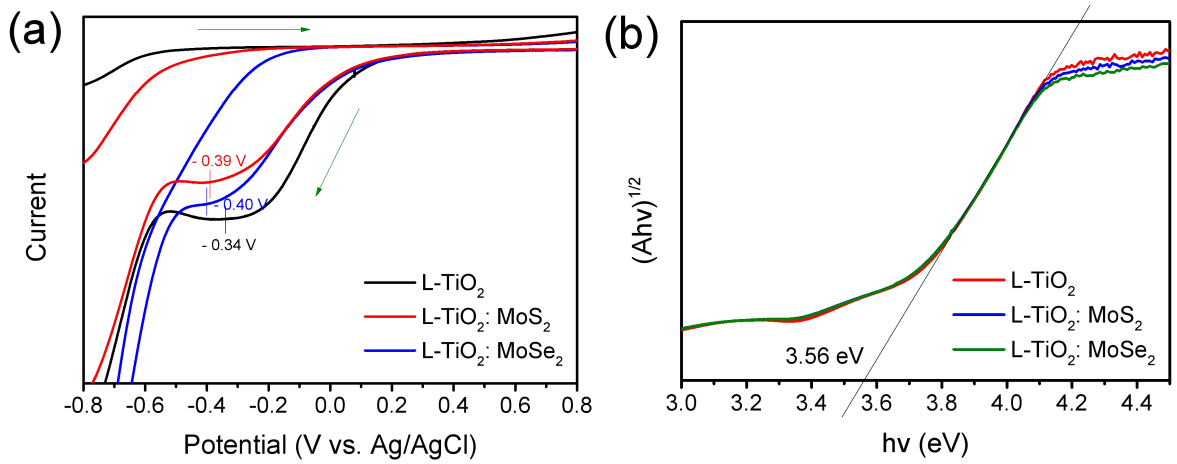

Fig. S10 (a) CV curves and (b) UV-vis spectra of L-TiO_2, L-TiO_2:MoS_2 and L-TiO_2:$MoSe_2$ films.

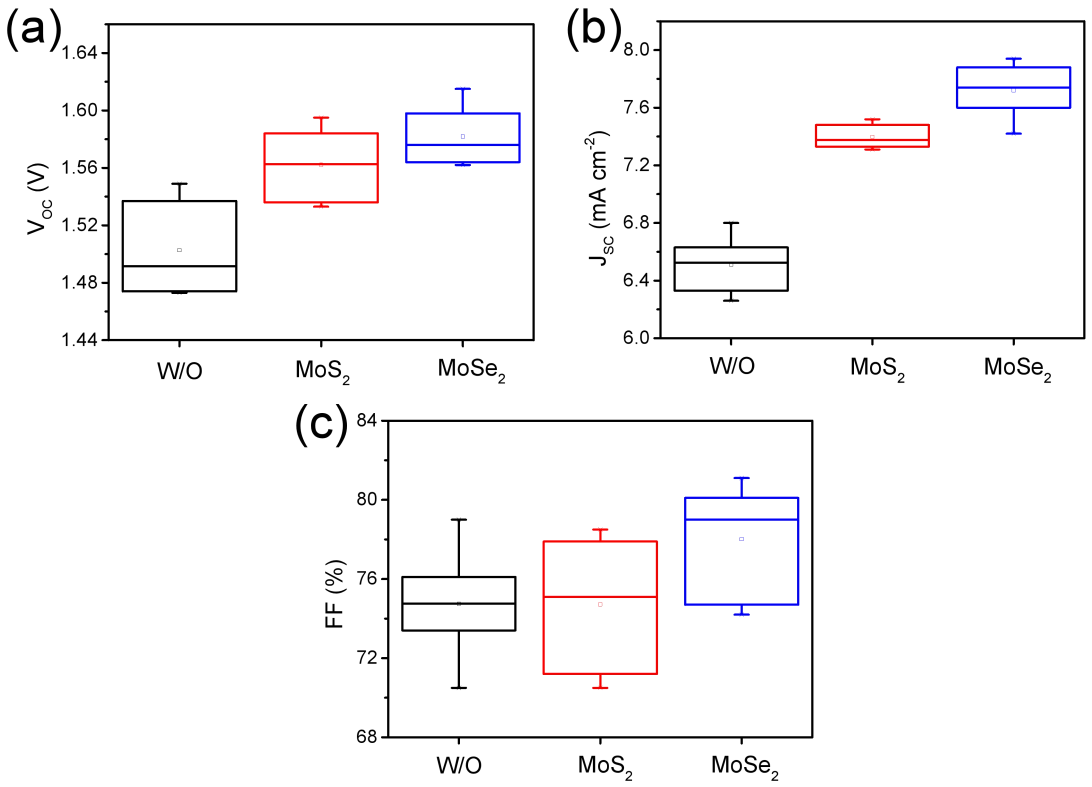

Fig. S11 The statistical distribution of (a) V_{oc}, (b) J_{sc} and (c) *FF* for 10 individual devices.

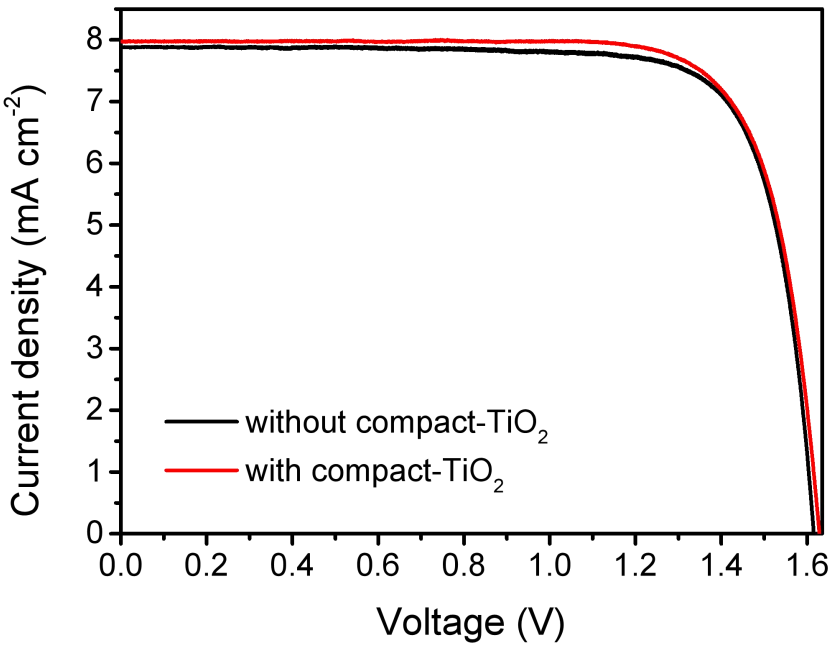

Fig. S12 The *J-V* curves of solar cells with and without compact-TiO_2 layer.

Table S1 The comparison of photovoltaic parameters for state-of-the-art inorganic $CsPbBr_3$ PSCs.

devices	J_{sc} (mA cm^{-2})	PCE (%)	*FF* (%)	V_{oc} (V)	Ref.
FTO/*L*-TiO_2:$MoSe_2$/$CsPbBr_3$/C	**7.88**	**10.02**	**78.7**	**1.615**	**This work**
FTO/*c*-TiO_2/*m*-TiO_2/$CsPbBr_3$/PTAA/Au	6.70	6.20	73.0	1.25	S1
FTO/*c*-TiO_2/*m*-TiO_2/$CsPbBr_3$/C	5.70	5.00	68.0	1.29	S2
FTO/ZnO/$CsPbBr_3$-$CsPb_2Br_5$/Spiro-OMeTAD/Au	6.17	6.81	77.2	1.43	S3
FTO/*c*-TiO_2/*m*-TiO_2/$CsPbBr_3$/Spiro-OMeTAD/Au	6.52	6.05	69.0	1.34	S4
ITO/ZnO/$CsPbBr_3$/Spiro-OMeTAD/Au	6.15	5.98	70.51	1.38	S5
FTO/TiO_2/CQD-$CsPbBr_3$ IO/Spiro-OMeTAD/Au	11.34	8.29	69.0	1.06	S6
FTO/*c*-TiO_2/*m*-TiO_2/$CsPbBr_3$/C	7.4	6.7	73.0	1.24	S7
FTO/*c*-TiO_2/$CsPbBr_3$/C	6.46	5.86	68.04	1.34	S8
FTO/mp-TiO_2/$CsPbBr_3$/PTAA/Au	6.16	5.72	73	1.28	S9
FTO/*c*-TiO_2/*m*-TiO_2/GQDs/$CsPbBr_3$/C	8.12	9.72	82.1	1.458	S10
FTO/*c*-TiO_2/*m*-TiO_2/Sm^{3+}-$CsPbBr_3$/C	7.48	10.14	85.1	1.594	S11
FTO/SnO_2/$CsPbBr_3$/N-CQDs/C	7.87	10.71	80.1	1.622	S12
FTO/*c*-TiO_2/*m*-TiO_2/Sm^{3+}-$CsPbBr_3$/Cu(Cr,Ba)O_2/C	7.81	10.79	85.5	1.615	S13
FTO/*c*-TiO_2/*m*-TiO_2/$CsPbBr_3$/$CuInS_2$/ZnS	7.73	10.85	86.3	1.626	S14
FTO/*c*-TiO_2/*m*-TiO_2/Sr^{2+}-$CsPbBr_3$/C	7.71	9.63	81.1	1.54	S15
FTO/*c*-TiO_2/*m*-TiO_2/Rb^{+}-$CsPbBr_3$/C	7.73	9.86	82.2	1.552	S16
FTO/*c*-TiO_2/*m*-TiO_2/GQDs/$CsPbBr_3$/MnS/C	8.28	10.45	83	1.52	S17
FTO/*c*-TiO_2/*m*-TiO_2/$CsPbBr_3$/Spiro-OMeTAD/Ag	6.4	6.3	72	1.37	S18
FTO/TiO_2/$CsPbBr_3$/C	7.48	6.12	68.8	1.19	S19

FTO/*c*-TiO_2/$CsPbBr_3$/C	6.89	8.11	79	1.49	S20
FTO/*c*-TiO_2/PTI-$CsPbBr_3$/spiro-OMeTAD/Ag	9.78	10.91	74.47	1.498	S21
FTO/*c*-TiO_2/*m*-TiO_2/GQDs/$CsPbBr_3$/P3HT/C	7.02	6.49	68	1.36	S22
FTO/*c*-TiO_2/SnO_2/$CsPbBr_3$/CuPc/C	8.24	8.79	81.4	1.31	S23
FTO/*c*-TiO_2/$CsPbBr_3$/C	7.37	9.35	82.2	1.545	S24
FTO/*c*-TiO_2/$CsPbBr_3$/Ti_3C_2-MXene/C	8.54	9.01	73.08	1.444	S25
FTO/*c*-TiO_2/*m*-TiO_2/Sn^{2+}-$CsPbBr_3$/C	7.66	8.63	82.22	1.37	S26
FTO/*c*-TiO_2/*m*-TiO_2/$CsPbBr_3$/C	7.40	7.37	84.1	1.22	S27
FTO/TiO_2/$CsPb_{0.998}Co_{0.002}Br_3$/Spiro-OMeTAD/Au	7.45	8.57	84.84	1.357	S28
FTO/*c*-TiO_2/$CsPbBr_3$/$CsPbBr_3$-$CsPb_2Br_5$/$CsPbBr_3$-Cs_4PbBr_6/C	9.26	10.17	75.39	1.461	S29
FTO/*c*-TiO_2/$CsPbBr_3$/spiro-OMeTAD/Au	6.97	6.95	78.5	1.27	S30
FTO/*c*-TiO_2/*m*-TiO_2/*m*-ZrO_2/$CsPbBr_3$/m-carbon	7.75	8.2	73.52	1.44	S31
FTO/*c*-TiO_2/$CsPbBr_3$–$CsPb_2Br_5$/spiro-OMeTAD/Ag	8.48	8.34	75.9	1.296	S32
FTO/*c*-TiO_2/$CsPbBr_3$/spiro-OMeTAD/Au	5.6	5.4	62	1.5	S33

Table S2 Summary of the trap density and mobility in L-TiO_2 with and without TMDCs QDs under different conditions.

ETL	Conditions	Trap density (cm^{-3})	Mobility ($cm^2\ V^{-1}\ s^{-1}$)
L-TiO_2	dark	9.13×10^{17}	3.48×10^{-4}
	illumination	8.75×10^{17}	3.66×10^{-4}
L-TiO_2:MoS_2	dark	7.27×10^{17}	5.34×10^{-4}
	illumination	3.04×10^{17}	7.30×10^{-4}
L-TiO_2:$MoSe_2$	dark	6.81×10^{17}	6.36×10^{-4}
	illumination	2.37×10^{17}	8.86×10^{-4}

Table S3. TRPL decay parameters of various L-TiO_2/$CsPbBr_3$ films with and without TMDCs QDs.

ETLs	τ_1 (ns)	a_1	τ_2 (ns)	a_2	τ_{ave} (ns)
L-TiO_2	1.436	37.86%	11.753	62.14%	3.158
L-TiO_2:MoS_2	1.212	57.65%	10.338	42.35%	1.935
L-TiO_2:$MoSe_2$	0.1383	68.62%	5.660	31.38%	0.199

References

S1 M. Kulbak, S. Gupta, N. Kedem, I. Levine, T. Bendikov, G. Hodes and D. Cahen, *J. Phys. Chem. Lett.*, 2016, **7**, 167–172.

S2 X. Chang, W. Li, L. Zhu, H. Liu, H. Geng, S. Xiang, J. Liu and H. Chen, *ACS Appl. Mater. Interfaces*, 2016, **8**, 33649–33655.

S3 X. Zhang, Z. Jin, J. Zhang, D. Bai, H. Bian, K. Wang, J. Sun, Q. Wang and S. F. Liu, *ACS Appl. Mater. Interfaces*, 2018, **10**, 7145–7154.

S4 K. C. Tang, P. You and F. Yan, *Sol. RRL*, 2018, **2**, 1800075.

S5 W. Chen, J. Zhang, G. Xu, R. Xue, Y. Li, Y. Zhou, J. Hou and Y. Li, *Adv. Mater.*, 2018, **30**, 1800855.

S6 S. Zhou, R. Tang and L. Yin, *Adv. Mater.*, 2017, **29**, 1703682.

S7 J. Liang, C. Wang, Y. Wang, Z. Xu, Z. Lu, Y. Ma, H. Zhu, Y. Hu, C. Xiao, X. Yi, G. Zhu, H. Lv, L. Ma, T. Chen, Z. Tie, Z. Jin and J. Liu, *J. Am. Chem. Soc.*, 2016, **138**, 15829–15832.

S8 P. Teng, X. Han, J. Li, Y. Xu, L. Kang, Y. Wang, Y. Yang and T. Yu, *ACS Appl. Mater. Interfaces*, 2018, **10**, 9541–9546.

S9 M. Kulbak, D. Cahen and G. Hodes, *J. Phys. Chem. Lett.*, 2015, **6**, 2452–2456.

S10 J. Duan, Y. Zhao, B. He and Q. Tang, *Angew. Chem. Int. Ed.*, 2018, **57**, 3787–3791.

S11 J. Duan, Y. Zhao, X. Yang, Y. Wang, B. He and Q. Tang, *Adv. Energy Mater.*, 2018, **8**, 1802346.

S12 Y. Zhao, J. Duan, Y. Wang, X. Yang and Q. Tang, *Nano Energy*, 2020, **67**, 104286.

S13 J. Duan, Y. Zhao, Y. Wang, X. Yang and Q. Tang, *Angew. Chem. Int. Ed.*, 2019, **58**, 16147–16151.

S14 J. Duan, Y. Wang, X. Yang and Q. Tang, *Angew. Chem. Int. Ed.*, 2020, DOI:10.1002/anie.202000199.

S15 Y. Zhao, Y. Wang, J. Duan, X. Yang and Q. Tang, *J. Mater. Chem. A*, 2019, **7**, 6877–6882.

S16 Y. Li, J. Duan, H. Yuan, Y. Zhao, B. He and Q. Tang, *Sol. RRL*, 2018, **2**, 1800164.

S17 X. Li, Y. Tan, H. Lai, S. Li, Y. Chen, S. Li, P. Xu and J. Yang, *ACS Appl. Mater. Interfaces*, 2019, **11**, 29746–29752.

S18 H. Wang, Y. Wu, M. Ma, S. Dong, Q. Li, J. Du, H. Zhang and Q. Xu, *ACS Appl. Energy Mater.*, 2019, **2**, 2305–2312.

S19 X. Cao, G. Zhang, L. Jiang, Y. Cai, Y. Gao, W. Yang, X. He, Q. Zeng, G. Xing, Y. Jia and J. Wei, *ACS Appl. Mater. Interfaces*, 2019, **12**, 5925–5931.

S20 X. Wan, Z. Yu, W. Tian, F. Huang, S. Jin, X. Yang, Y.-B. Cheng, A. Hagfeldt and L. Sun, *J. Energy Chem.*, 2020, **46**, 8–15.

S21 G. Tong, T. Chen, H. Li, L. Qiu, Z. Liu, Y. Dang, W. Song, L. K. Ono, Y. Jiang and Y. Qi, *Nano Energy*, 2019, **65**, 104015.

S22 G. Wang, W. Dong, A. Gurung, K. Chen, F. Wu, Q. He, R. Pathak and Q. Qiao, *J. Power Sources*, 2019, **432**, 48–54.

S23 X. Liu, X. Tan, Z. Liu, H. Ye, B. Sun, T. Shi, Z. Tang and G. Liao, *Nano Energy*, 2019, **56**, 184–195.

S24 T. Xiang, Y. Zhang, H. Wu, J. Li, L. Yang, K. Wang, J. Xia, Z. Deng, J. Xiao, W. Li, Z. Ku, F. Huang, J. Zhong, Y. Peng and Y.-B. Cheng, *Sol. Energy Mater. Sol. Cells*, 2019, 110317.

S25 T. Chen, G. Tong, E. Xu, H. Li, P. Li, Z. Zhu, J. Tang, Y. Qi and Y. Jiang, *J. Mater. Chem. A*, 2019, **7**, 20597–20603.

S26 H. Guo, Y. Pei, J. Zhang, C. Cai, K. Zhou and Y. Zhu, *J. Mater. Chem. C*, 2019, **7**, 11234–11243.

S27 D. Huang, P. Xie, Z. Pan, H. Rao and X. Zhong, *J. Mater. Chem. A*, 2019, **7**, 22420–22428.
S28 D. Wang, W. Li, Z. Du, G. Li, W. Sun, J. Wu and Z. Lan, *J. Mater. Chem. C*, 2020, **8**, 1649–1655.
S29 G. Tong, T. Chen, H. Li, W. Song, Y. Chang, J. Liu, L. Yu, J. Xu, Y. Qi and Y. Jiang, *Sol. RRL*, 2019, **3**, 1900030.
S30 J. Lei, F. Gao, H. Wang, J. Li, J. Jiang, X. Wu, R. Gao, Z. Yang and S. (Frank) Liu, *Sol Energy Mater. Solar Cells*, 2018, **187**, 1–8.
S31 I. Poli, J. Baker, J. McGettrick, F. De Rossi, S. Eslava, T. Watson and P. J. Cameron, *J. Mater. Chem. A*, 2018, **6**, 18677–18686.
S32 H. Li, G. Tong, T. Chen, H. Zhu, G. Li, Y. Chang, L. Wang and Y. Jiang, *J. Mater. Chem. A*, 2018, **6**, 14255–14261.
S33 Q. A. Akkerman, M. Gandini, F. Di Stasio, P. Rastogi, F. Palazon, G. Bertoni, J. M. Ball, M. Prato, A. Petrozza and L. Manna, *Nat Energy*, 2017, **2**, 16194.